Alternative "Bases" for Gradient-Based Optimization of Parameterized FM Radar Waveforms

Bahozhoni White, Matthew B. Heintzelman, Shannon D. Blunt
Radar Systems Lab (RSL), University of Kansas, Lawrence, KS

Background

- Spectrally-shaped **random FM** (RFM) waveforms:
  - Are amendable to high power transmitters (constant amplitude & continuous phase)
  - Can be designed to achieve low sidelobes
  - Have been experimentally demonstrated for a variety of applications

- **Parameterized** version of **RFM** readily permit gradient-based **optimization**
  - Extensible to joint optimization across waveform sets
  - Preserve transmitter-amenable attributes (under certain conditions)

Motivation

- Here we consider other parameterized structures to examine the impact of choice in "basis"
  - Due to **requirement for over-sampling** (relative to 3-dB bandwidth) to ensure spectral containment, these structures are not true bases => hence, **quasi-bases**
- We specifically examine **2nd-order polyphase-coded FM** (PCFM) and **Fourier** quasi-bases, along with **1st-order PCFM** as a baseline **[1]**
  - These are chosen because we expect the ensuing RFM waveforms generated from each to possess different attributes

[1] P.S. Tan, J. Jakabosky, J. Stiles, S. Blunt, "Higher-order implementations of polyphase-coded FM radar waveforms," ***IEEE Trans. Aerospace & Electronic Systems*****, vol. 55, no. 6, pp. 2850-2870, Dec. 2019.**

Parameterized FM Waveforms

Discretized FM Waveform Structure

- Define an arbitrary FM waveform (hence continuous) as

$$s(t\,;\mathbf{x}) = \exp(\,j\,\phi(t\,;\mathbf{x}))$$

in which **[2]**

$$\phi(t\,;\mathbf{x}) = \sum_{n=1}^{N} \alpha_n\, b_n(t) \qquad\qquad \mathbf{x} = [\alpha_1\ \alpha_2 \cdots \alpha_N\,]^T$$

permits a parameterized combining of **continuous phase functions** $b_n(t)$

- Properly discretizing these phase functions to ensure **sufficient spectral containment** then yields

$$\mathbf{s} = \exp(\,j\,\mathbf{B}\mathbf{x}) \qquad\qquad \mathbf{B} = [\mathbf{b}_1\ \mathbf{b}_2\ \cdots \mathbf{b}_N\,] \longrightarrow M{\times}N \text{ for } M > N$$

[2] C.A. Mohr, P.M. McCormick, C.A. Topliff, S.D. Blunt, J.M. Baden, "Gradient-based optimization of PCFM radar waveforms," *IEEE Trans. Aerospace & Electronic Systems*, vol. 57, no. 2, pp. 935-956, Apr. 2021.

1st-Order PCFM

- The **1st-order PCFM** implementation conforms to this structure via

$$\phi_1(t;\mathbf{x}) = \int_0^t g(\tau) * \left[\sum_{n=1}^{N} \alpha_n \, \delta(t-(n-1)\,T_\mathrm{I}) \right] d\tau$$

shaping filter
(generally rectangular)

impulse train with separation T_I

so that the corresponding phase functions are

$$b_n(t) = \int_0^t g(\tau-(n-1)T_\mathrm{I})\, d\tau = \begin{cases} 0, & 0 \le t < (n-1)T_\mathrm{I} \\ (t-(n-1)\,T_\mathrm{I})/T_\mathrm{I}, & (n-1)T_\mathrm{I} \le t < nT_\mathrm{I} \\ 1, & nT_\mathrm{I} \le t \le NT_\mathrm{I} \end{cases}$$

1st-Order PCFM

- The **1st-order PCFM** implementation conforms to this structure via

$$\phi_1(t;\mathbf{x}) = \int_0^t g(\tau) * \left[\sum_{n=1}^{N} \alpha_n \, \delta(t-(n-1)\,T_{\mathrm{I}})\right] d\tau$$

shaping filter
(generally rectangular)

impulse train with separation T_{I}

so that the corresponding phase functions are

$$b_n(t) = \int_0^t g(\tau-(n-1)T_{\mathrm{I}})\, d\tau = \begin{cases} 0, & 0 \le t < (n-1)T_{\mathrm{I}} \\ \boxed{(t-(n-1)\,T_{\mathrm{I}})/T_{\mathrm{I}},} & (n-1)T_{\mathrm{I}} \le t < nT_{\mathrm{I}} \\ 1, & nT_{\mathrm{I}} \le t \le NT_{\mathrm{I}} \end{cases}$$

linear ramp

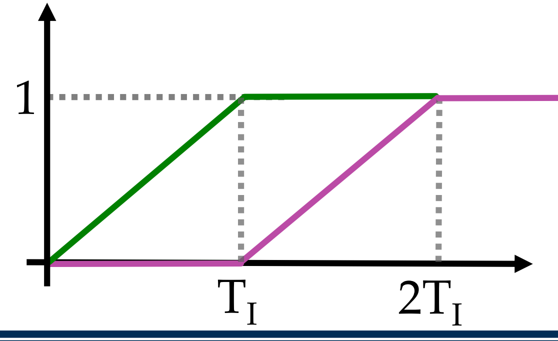

2^{nd}-Order PCFM

- The **2^{nd}-order PCFM** implementation involves an additional integration so that

$$\phi_2(t;\mathbf{x}) = \bar{\omega}_2\, t + \int_0^t \int_0^\tau \sum_{n=1}^{N} \alpha_n \, g\left(t-(n-1)T_\mathrm{I}\right)\right) \, d\tau' \, d\tau$$

results in the phase functions

$$b_n(t) = \int_0^t \int_0^\tau g(\tau' - (n-1)T_\mathrm{I})\, d\tau' \, d\tau$$

$$= \begin{cases} 0, & 0 \le t < (n-1)T_\mathrm{I} \\ t^2/(2\,T_\mathrm{I}^2) - (n-1)\,t/\,T_\mathrm{I} + (n-1)^2/2, & (n-1)\,T_\mathrm{I} \le t < n\,T_\mathrm{I} \\ t\,/\,T_\mathrm{I} + 1/2 - n & nT_\mathrm{I} \le t \le N\,T_\mathrm{I} \end{cases}$$

2$^{\text{nd}}$-Order PCFM

- The **2$^{\text{nd}}$-order PCFM** implementation involves an additional integration so that

$$\phi_2(t;\mathbf{x}) = \bar{\omega}_2\, t + \int_0^t \int_0^\tau \sum_{n=1}^{N} \alpha_n\; g\big(t-(n-1)T_{\mathrm{I}}\big)\big)\; d\tau'\, d\tau$$

results in the phase functions

$$b_n(t) = \int_0^t \int_0^\tau g\big(\tau' - (n-1)T_{\mathrm{I}}\big)\, d\tau'\, d\tau$$

quadratic

$$= \begin{cases} 0, & 0 \le t < (n-1)T_{\mathrm{I}} \\ \boxed{t^2/(2\,T_{\mathrm{I}}^2) - (n-1)\,t/\,T_{\mathrm{I}} + (n-1)^2/2,} & (n-1)T_{\mathrm{I}} \le t < n\,T_{\mathrm{I}} \\ \boxed{t\,/\,T_{\mathrm{I}} + 1/2 - n} & nT_{\mathrm{I}} \le t \le N\,T_{\mathrm{I}} \end{cases}$$

linear ramp

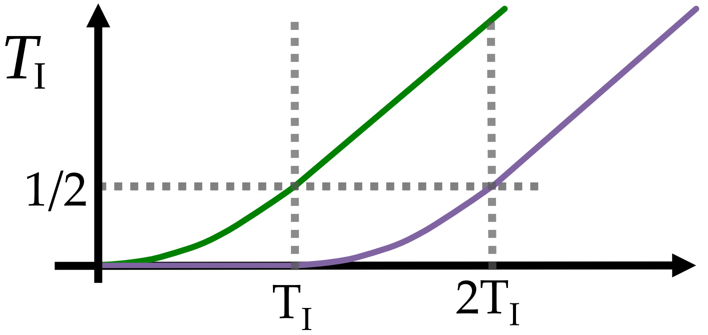

2^{nd}-Order PCFM

- The **2^{nd}-order PCFM** implementation involves an additional integration so that

$$\phi_2(t;\mathbf{x}) = \bar{\omega}_2\, t + \int_0^t \int_0^\tau \sum_{n=1}^{N} \alpha_n\, g(t-(n-1)T_{\mathrm{I}}))\; d\tau'\, d\tau$$

plus a frequency offset (becomes another column in **B**)

results in the phase functions

$$b_n(t) = \int_0^t \int_0^\tau g(\tau' - (n-1)T_{\mathrm{I}})\, d\tau'\, d\tau$$

$$= \begin{cases} 0, & 0 \le t < (n-1)T_{\mathrm{I}} \\ \boxed{t^2/(2\,T_{\mathrm{I}}^2) - (n-1)\,t/T_{\mathrm{I}} + (n-1)^2/2,} & (n-1)T_{\mathrm{I}} \le t < nT_{\mathrm{I}} \\ \boxed{t/T_{\mathrm{I}} + 1/2 - n} & nT_{\mathrm{I}} \le t \le N\,T_{\mathrm{I}} \end{cases}$$

quadratic

linear ramp

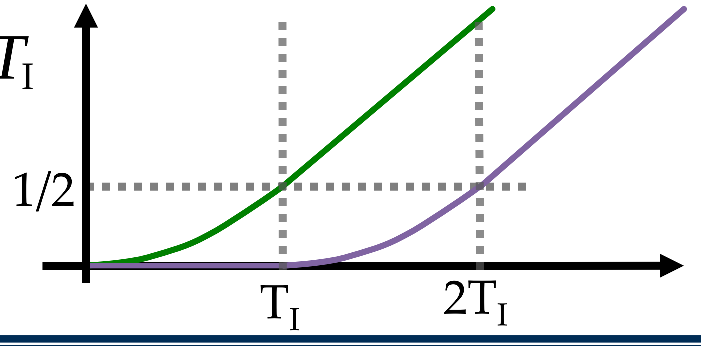

Fourier

- Finally, the **Fourier** implementation, which is what **CE-OFDM** employs, takes the form

$$\phi_{\mathrm{F}}(t;\mathbf{x}_{\mathrm{F}}) = \Re\left\{\sum_{n=1}^{N} \alpha_n \exp(j\,\omega_n t)\right\}$$

$$= \sum_{n=1}^{N} \Re\{\alpha_n\}\cos(\omega_n t) + \Im\{\alpha_n\}\sin(\omega_n t)$$

$$= \sum_{n=1}^{N} \alpha_{\mathrm{r},n}\cos(\omega_n t) + \alpha_{\mathrm{i},n}\sin(\omega_n t),$$

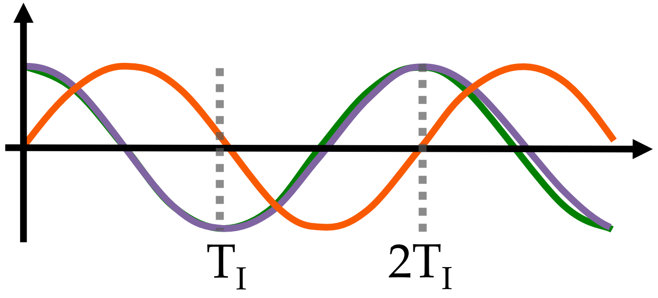

so that the **phase functions** are clearly $\cos(\omega_n t)$ and $\sin(\omega_n t)$

- Because this implementation possesses **double the phase functions**, we shall set N to be half that of the other two implementations for fair comparison.

Gradient-Based Optimization

Cost Function

- **Discretizing waveform** $s(t)$ as $\mathbf{s}$, the ensuing **autocorrelation** can be written as

$$\mathbf{r} = \mathbf{A}^H \left[\left(\mathbf{A}\bar{\mathbf{s}} \right) \odot \left(\mathbf{A}\bar{\mathbf{s}} \right)^* \right]$$

for $\bar{\mathbf{s}}$ the zero-padded version, $\mathbf{A}$ the DFT, and $\mathbf{A}^H$ the inverse DFT.

- By selecting the **mainlobe** and **sidelobe** regions using $\mathbf{w}_{\mathrm{ML}}$ and $\mathbf{w}_{\mathrm{SL}}$, the **generalized integrated sidelobe level** (GISL) cost function is

$$J_p = \frac{\left\| \mathbf{w}_{\mathrm{SL}} \odot \mathbf{r} \right\|_p^2}{\left\| \mathbf{w}_{\mathrm{ML}} \odot \mathbf{r} \right\|_p^2}$$

where $p = 2$ is the ISL metric and $p \to \infty$ is the PSL metric

Gradient-Based Optimization

- It was shown in [2] that the **gradient** of the GISL cost function is

$$\nabla_{\mathbf{x}} J_p = 4\, J_p\, \bar{\mathbf{B}}^T\, \Im\left\{ \bar{\mathbf{s}}^* \odot \left(\mathbf{A}^H \left[\mathbf{A} \left(\left[\frac{\mathbf{w}_{SL}}{\mathbf{w}_{SL}^T |\mathbf{r}|^p} - \frac{\mathbf{w}_{ML}}{\mathbf{w}_{ML}^T |\mathbf{r}|^p} \right] \odot |\mathbf{r}|^{(p-2)} \odot \mathbf{r} \right) \odot (\mathbf{A}\, \bar{\mathbf{s}}) \right] \right) \right\}$$

with $\bar{\mathbf{B}}$ having columns of zeros appended to agree with $\bar{\mathbf{s}}$.

- Gradient-descent **update** is then performed as

$$\mathbf{x}_i = \mathbf{x}_{i-1} + \mu_i \mathbf{q}_i \quad \text{for} \quad \mathbf{q}_i = \begin{cases} -\nabla_{\mathbf{x}} J_p(\mathbf{x}_{i-1}) & \text{when } i = 0 \\ -\nabla_{\mathbf{x}} J_p(\mathbf{x}_{i-1}) + \beta \mathbf{q}_{i-1} & \text{otherwise} \end{cases}$$

Backtracking

[2] C.A. Mohr, P.M. McCormick, C.A. Topliff, S.D. Blunt, J.M. Baden, "Gradient-based optimization of PCFM radar waveforms," *IEEE Trans. Aerospace & Electronic Systems*, vol. 57, no. 2, pp. 935-956, Apr. 2021.

Optimization Results

Initialization Mappings

- As noted in [2], the GISL cost function **does not** inherently **address spectral containment**.
- While a spectral constraint could be considered, we want to **focus solely** on the **behaviors** associated with these **quasi-bases**.
- Instead, we therefore use an initialization already possessing acceptable containment and rely on gradient-descent to stay in this local region.
- Hence, we initialize with **PRO-FM waveforms** [3] and then use least-squares (LS) in phase to map into the parameterization for each quasi-basis as

discretized phase of kth PRO-FM waveform

$$\boldsymbol{\phi}_{\mathrm{PRO},k} \xrightarrow{\mathrm{LS}\{\mathbf{B}_{\mathrm{1st}}\}} \mathbf{x}_{\mathrm{1st},k} \quad \Big| \quad \xrightarrow{\mathrm{LS}\{\mathbf{B}_{\mathrm{2nd}}\}} \mathbf{x}_{\mathrm{2nd},k} \quad \Big| \quad \xrightarrow{\mathrm{LS}\{\mathbf{B}_{\mathrm{F}}\}} \mathbf{x}_{\mathrm{F},k}$$

[2] C.A. Mohr, P.M. McCormick, C.A. Topliff, S.D. Blunt, J.M. Baden, "Gradient-based optimization of PCFM radar waveforms," *IEEE Trans. Aerospace & Electronic Systems*, vol. 57, no. 2, pp. 935-956, Apr. 2021.

[3] J. Jakabosky, S.D. Blunt, B. Himed, "Spectral-shape optimized FM noise radar for pulse agility," *IEEE Radar Conf.*, Philadelphia, PA, May 2016.

Convergence Behavior Comparison

- **Fourier** convergence
  - drops **~9 dB** in 10^3 iterations, then flatlines
- 1^{st} **order** convergence
  - drops **~6 dB** in 10^3 iterations, then gradually reduces another **4 dB** until 10^5
- 2^{nd} **order** convergence
  - Takes nearly 10^4 iterations before meaningful convergence takes hold, with only about **2 dB per decade** of iterations thereafter

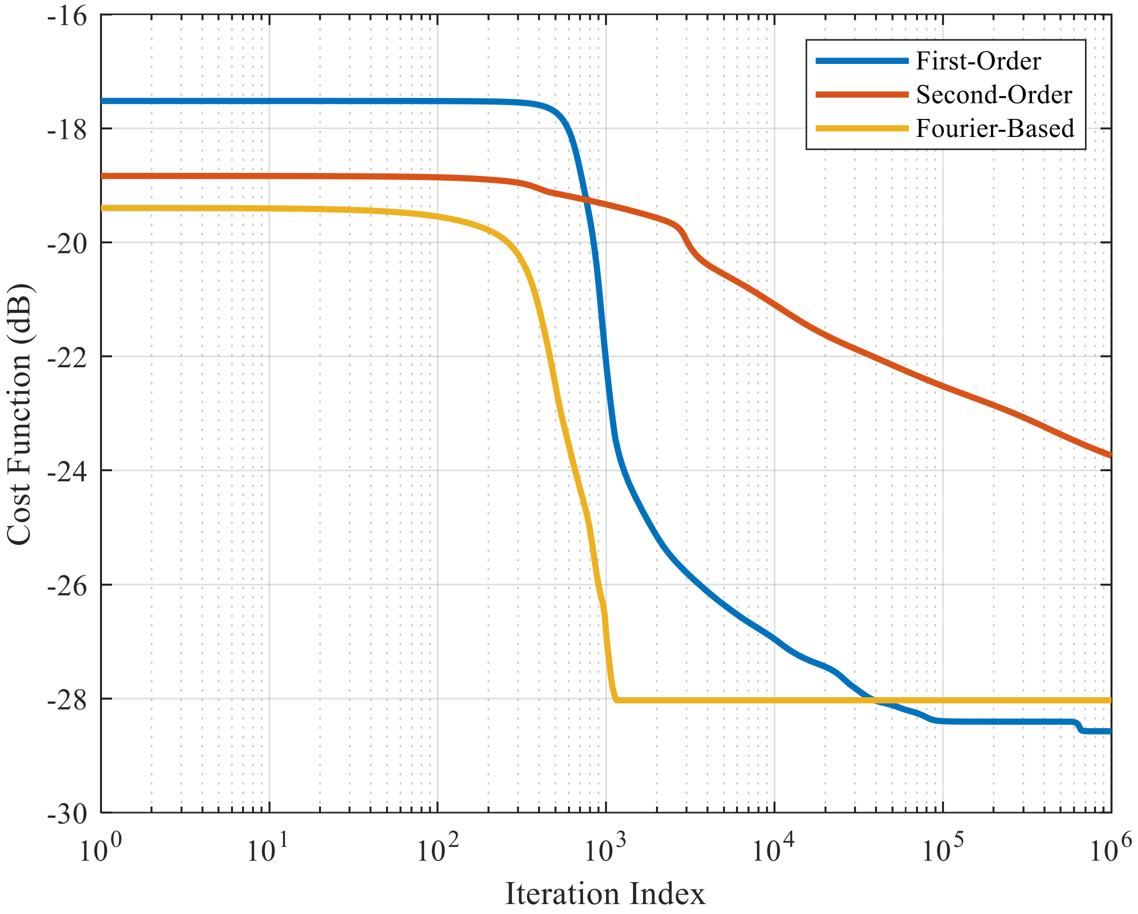

Convergence Behavior Comparison

- **Fourier** convergence
  - drops **~9 dB** in 10^3 iterations, then flatlines
- 1^{st} **order** convergence
  - drops **~6 dB** in 10^3 iterations, then gradually reduces another **4 dB** until 10^5
- 2^{nd} **order** convergence
  - Takes nearly 10^4 iterations before meaningful convergence takes hold, with only about **2 dB per decade** of iterations thereafter

subsequent analysis based on 9000 iterations

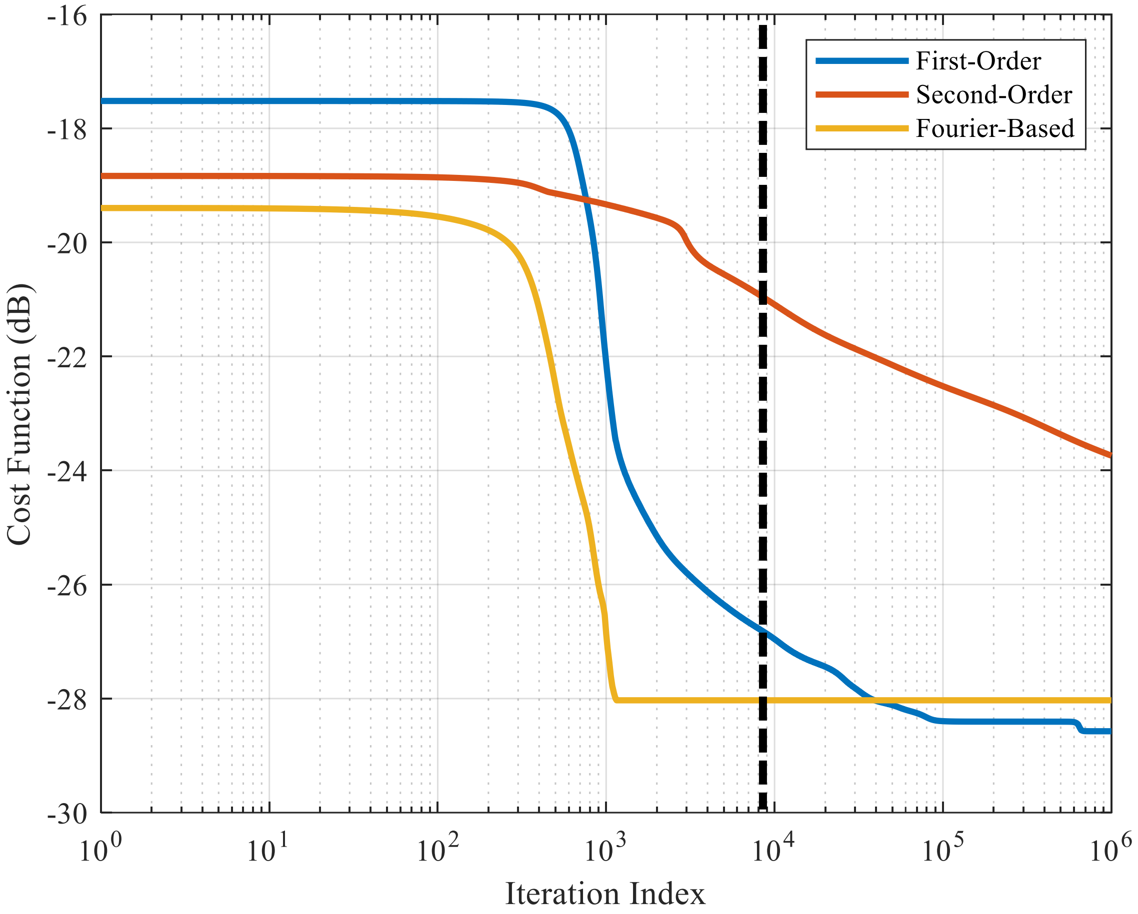

Optimized Autocorrelation Comparison

- Initializing with $K = 3000$ unique **PRO-FM** waveforms having $TB = 200$ and 4× oversampling
- LS mapping into each quasi-basis, then 9000 gradient-descent iterations
- **RMS** (per-pulse average) and **coherent** slow-time combining yield **similar outcomes** despite differences in convergence
  - RMS: Fourier ~1 dB below 1st order, which is ~4 dB below 2nd order

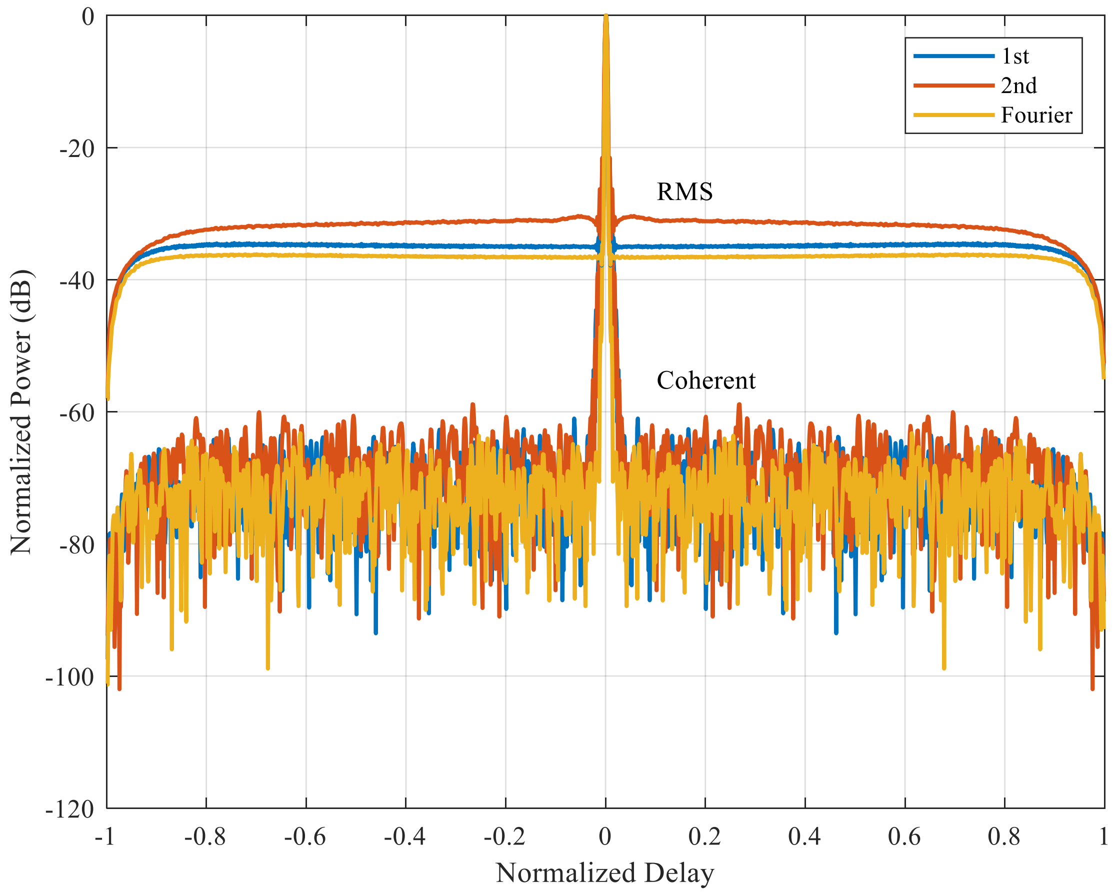

Optimized Autocorrelation Comparison

- Close-up on the mainlobe shows **shoulder lobe** roll-off due to initial super-Gaussian shaping for PRO-FM

- **Fourier** case has largely **suppressed** the initial shoulder lobes, while **1st** and **2nd** order **preserve** them to different degrees

- Local minima associated with this effect may **explain differing convergence rates**

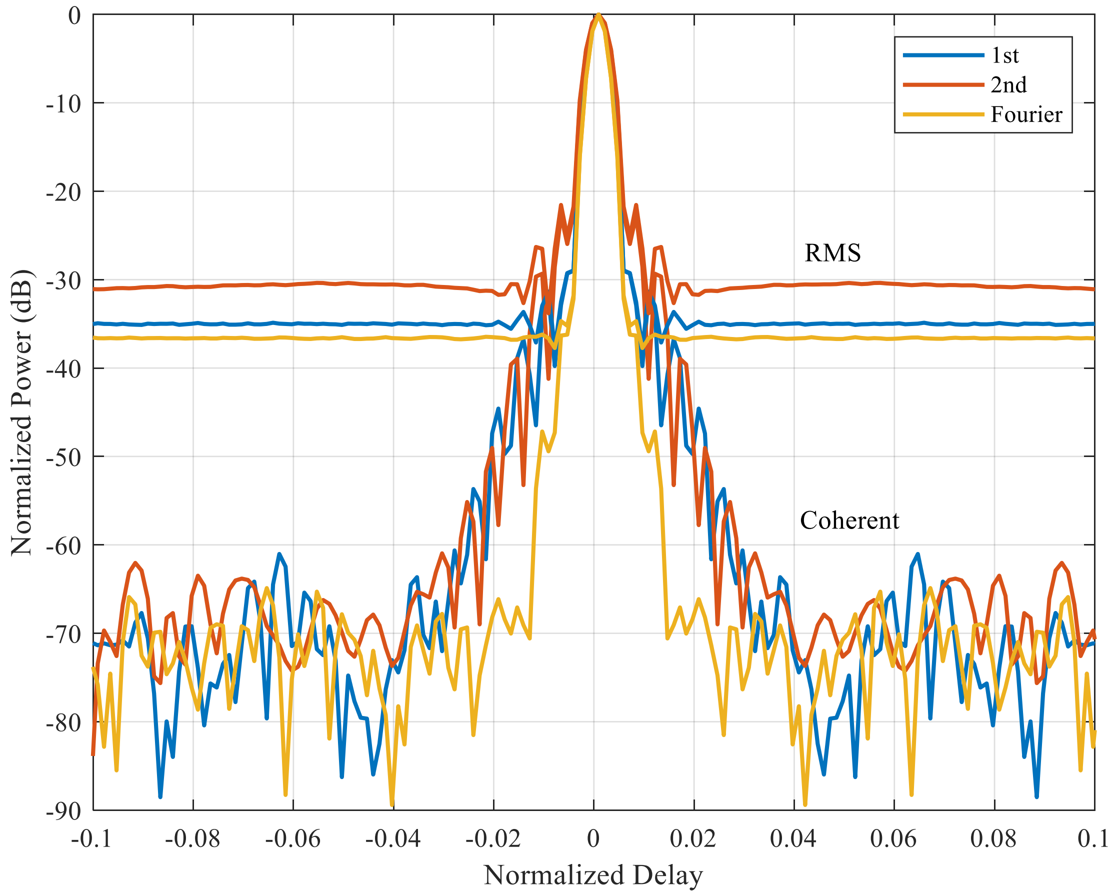

Optimized Autocorrelation Comparison

- Close-up on the mainlobe shows **shoulder lobe** roll-off due to initial super-Gaussian shaping for PRO-FM

- **Fourier** case has largely **suppressed** the initial shoulder lobes, while **1st** and **2nd** order **preserve** them to different degrees

- Local minima associated with this effect may **explain differing convergence rates**

- However, this attribute is also associated with better spectral containment

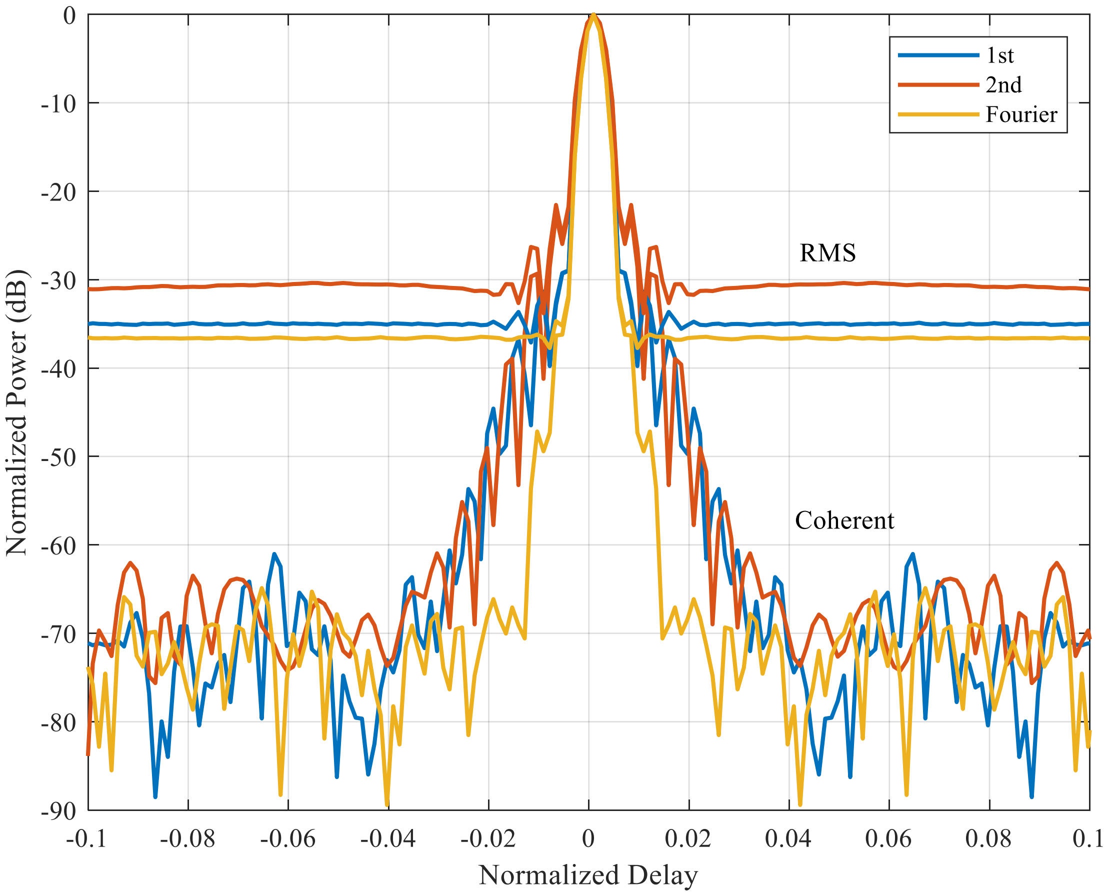

Power Spectral Density (PSD) Comparison

- Previous behavior is better understood after examining the resulting PSD for each case
  - Depicted for **single waveform, RMS average**, and **PRO-FM initialization** (average)

1st order quasi-basis

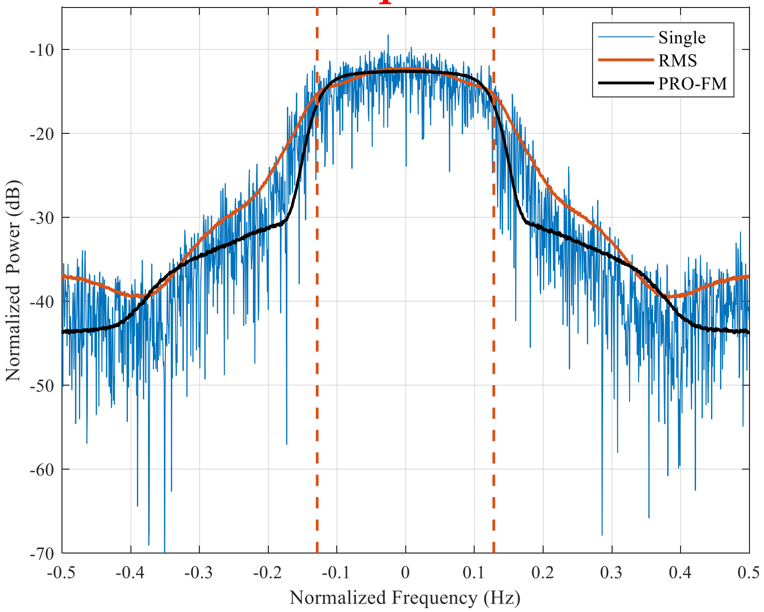

2nd order quasi-basis

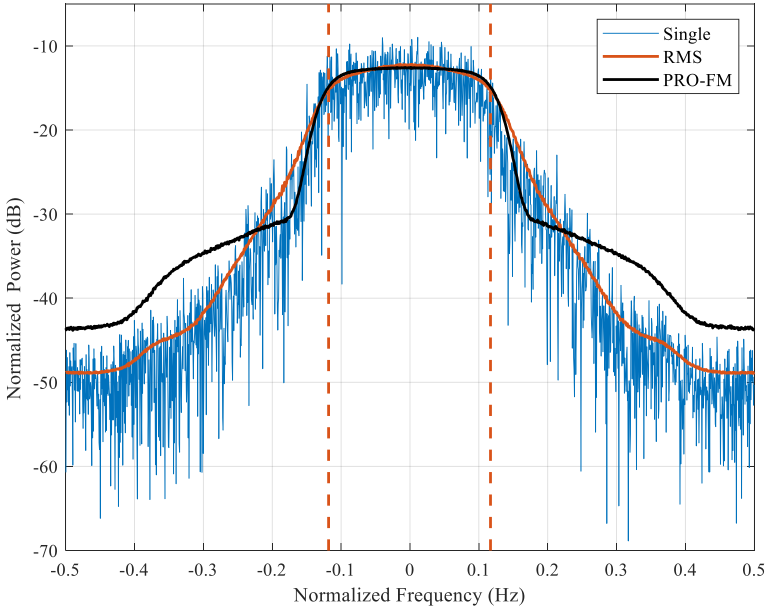

Fourier quasi-basis

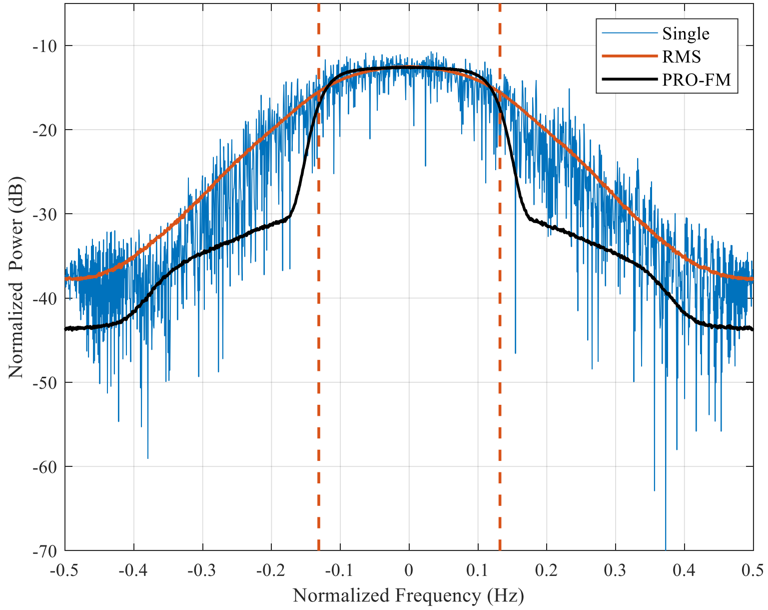

Power Spectral Density (PSD) Comparison

- Previous behavior is better understood after examining the resulting PSD for each case
  - Depicted for **single waveform, RMS average**, and **PRO-FM initialization** (average)

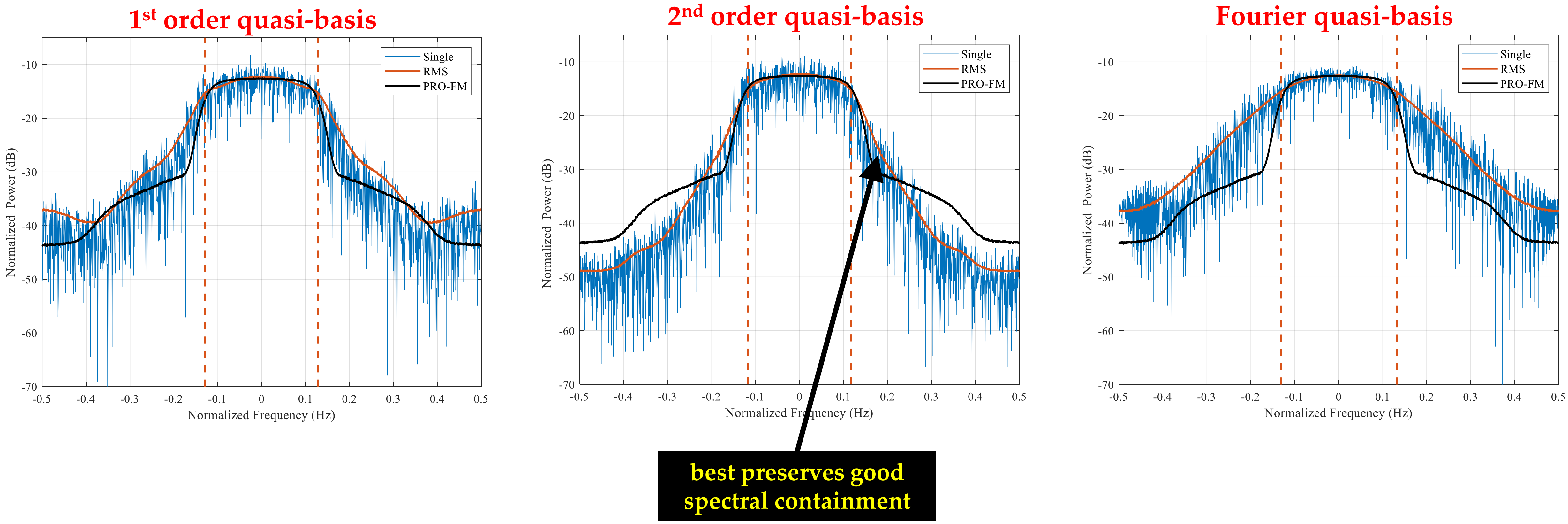

Power Spectral Density (PSD) Comparison

- Previous behavior is better understood after examining the resulting PSD for each case
  - Depicted for **single waveform, RMS average**, and **PRO-FM initialization** (average)

1st order quasi-basis

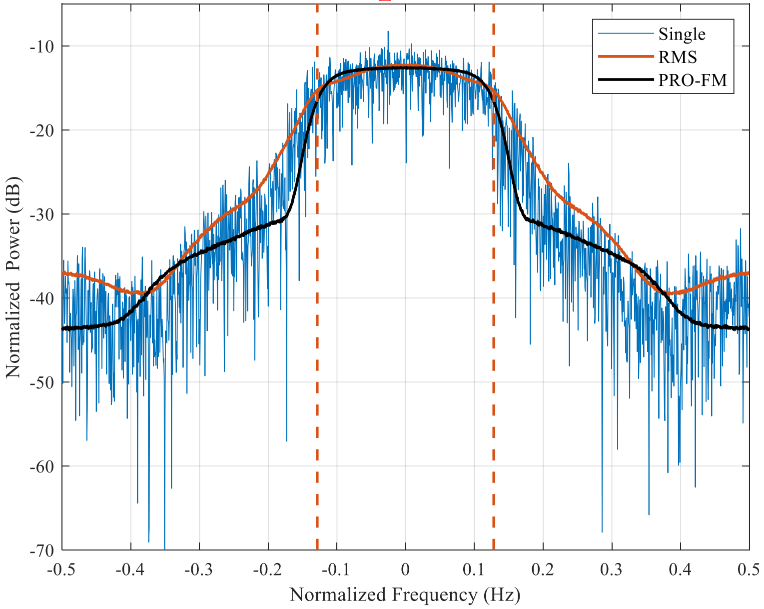

2nd order quasi-basis

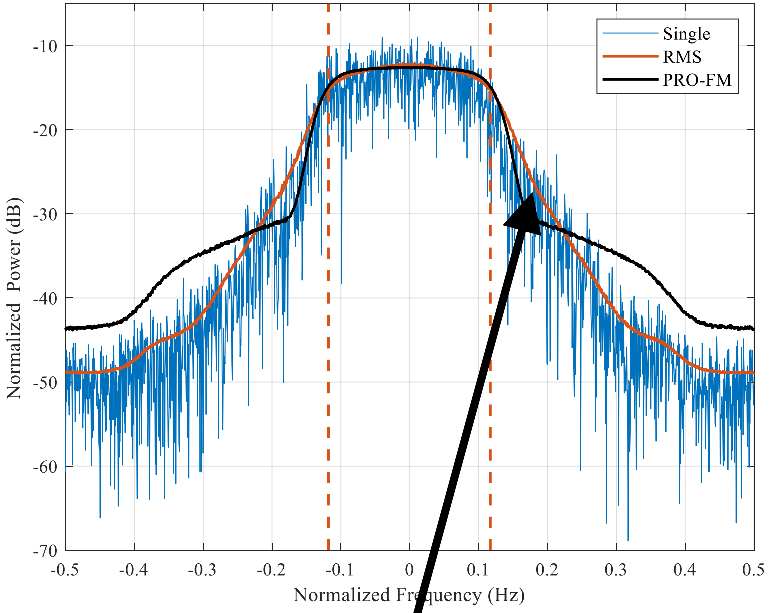

Fourier quasi-basis

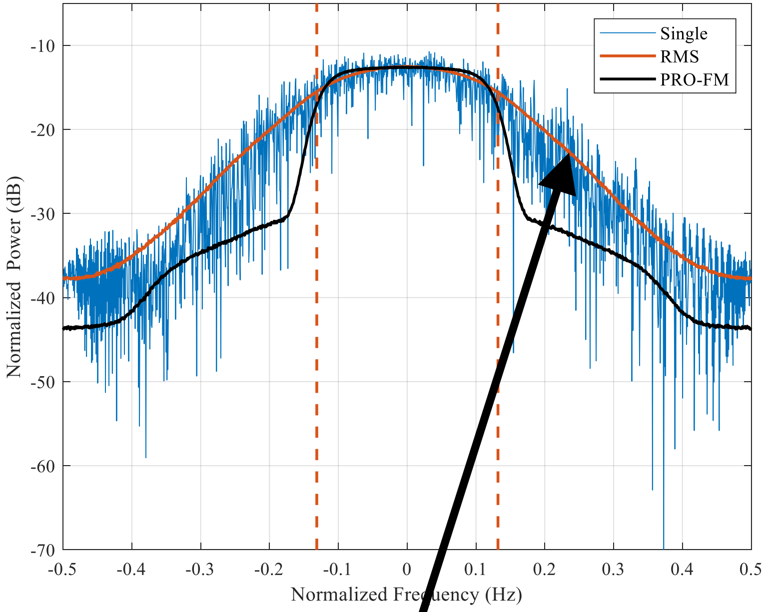

best preserves good spectral containment

tends toward Gaussian PSD, hence lower sidelobes

Power Spectral Density (PSD) Comparison

- Previous behavior is better understood after examining the resulting PSD for each case
  - Depicted for **single waveform, RMS average**, and **PRO-FM initialization** (average)

1st order quasi-basis

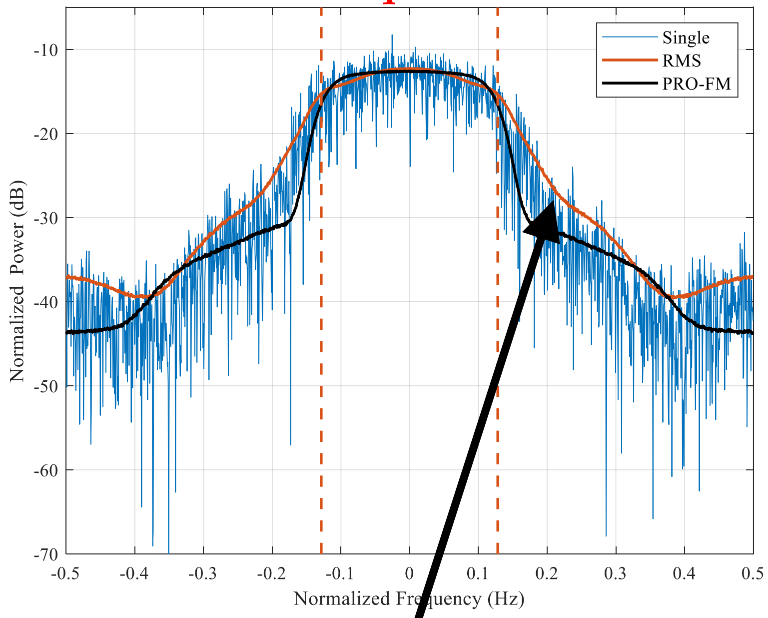

in between

2nd order quasi-basis

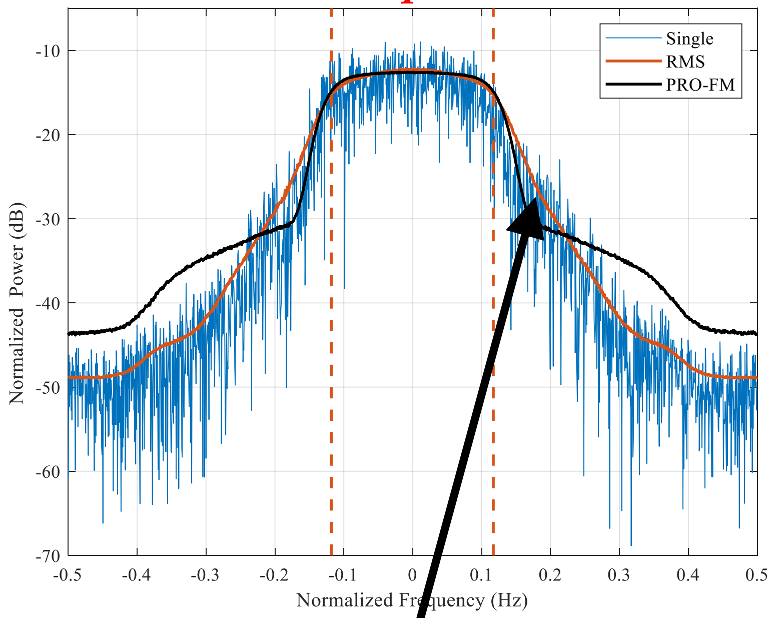

best preserves good spectral containment

Fourier quasi-basis

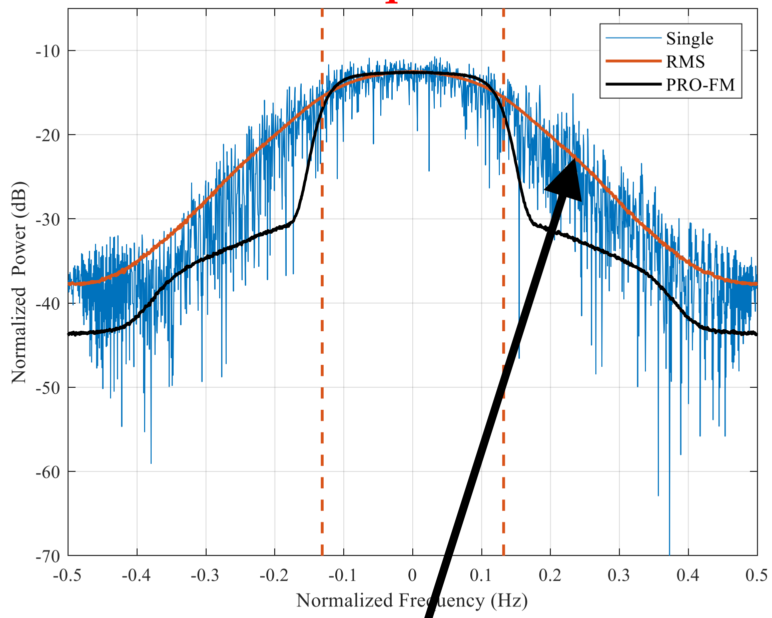

tends toward Gaussian PSD, hence lower sidelobes

Instantaneous Phase/Frequency Comparison

Instantaneous Phase $\phi(t)$

- All are **continuous** since they are FM
- 1st order is **piece-wise linear**
- 2nd order could realize LFM perfectly
- Fourier: infinitely differentiable => **smooth phase**

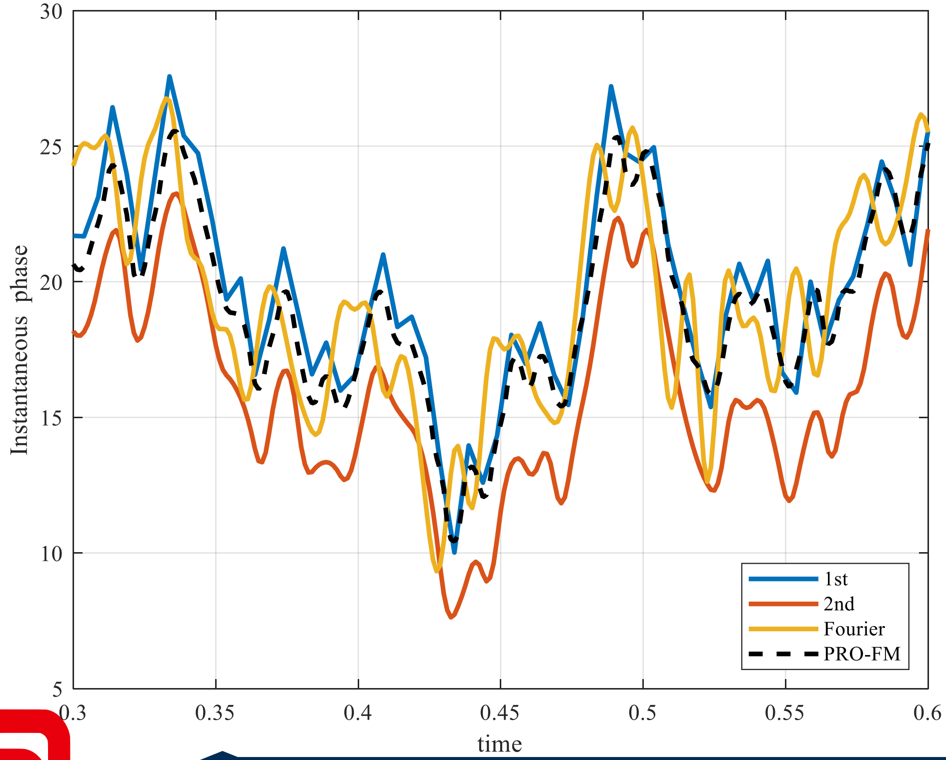

Instantaneous Frequency $d\phi(t)/dt$

- 1st order now has **discontinuities**
- 2nd order is piece-wise linear
- Fourier does show higher freq. excursions that conform to more gradual roll-off

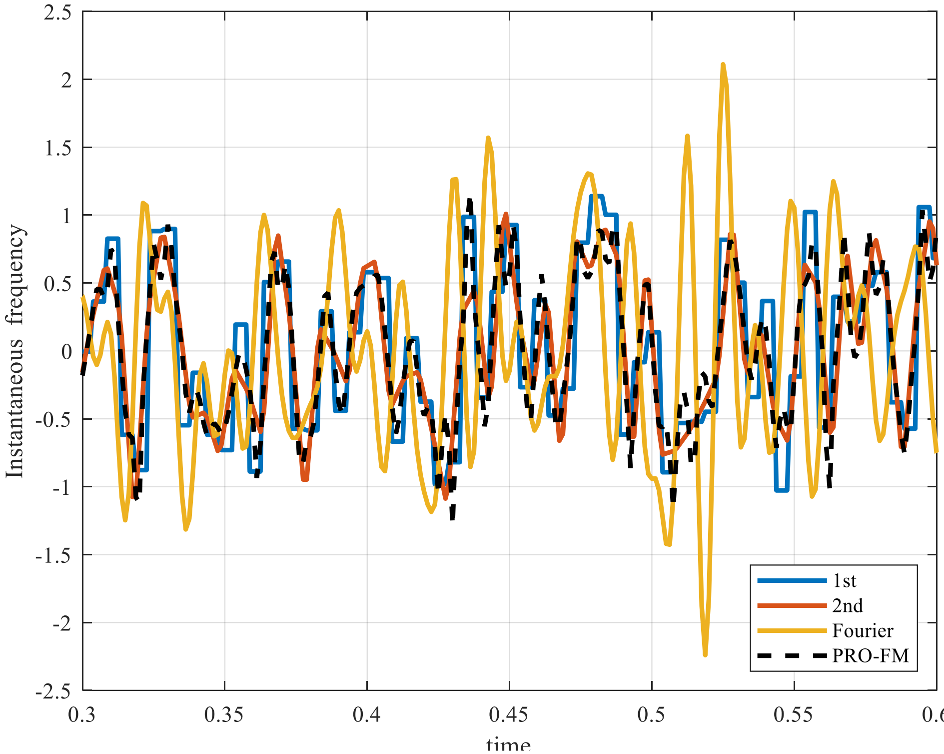

Experimental Results

Open-Air Measurements

- **Test Setup**
  - On roof of Nichols Hall on University of Kansas campus
  - Illuminating intersection of 23rd and Iowa streets
  - Interleaved waveforms to provide same scene for comparison
- **Test Parameters**
  - TB: 200
  - PRI: 22 μs
  - CPI: 198 ms
  - Center frequency: 3.45 GHz
- **Processing**
  - Simple projection-based clutter cancellation (since stationary platform)
  - Applied Taylor window (-35 dB) in Doppler

Range-Doppler Responses

- Different quasi-basis structures ⟶ Still physically realizable waveforms

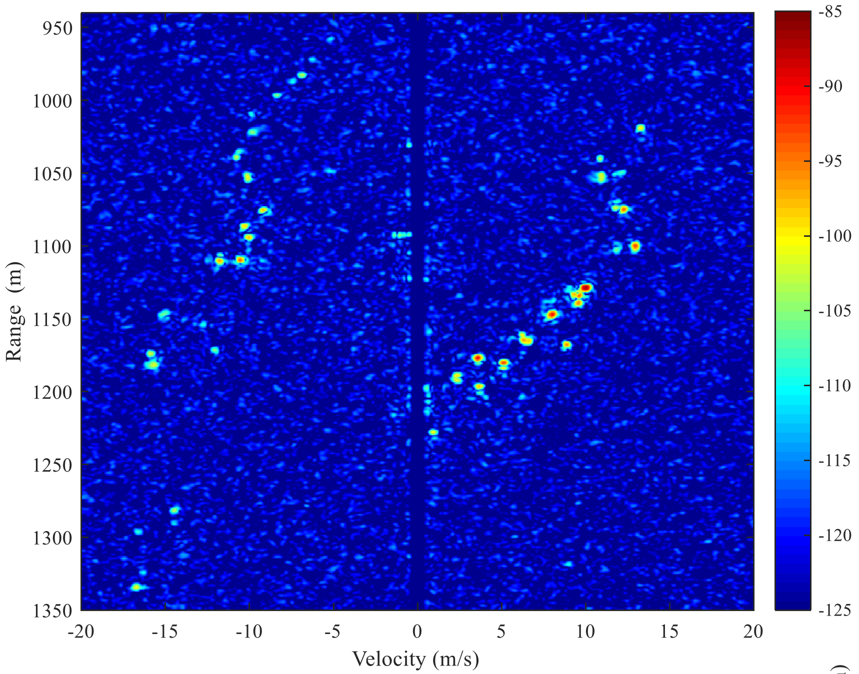

1st order quasi-basis

Not surprising, but good to confirm

2nd order quasi-basis

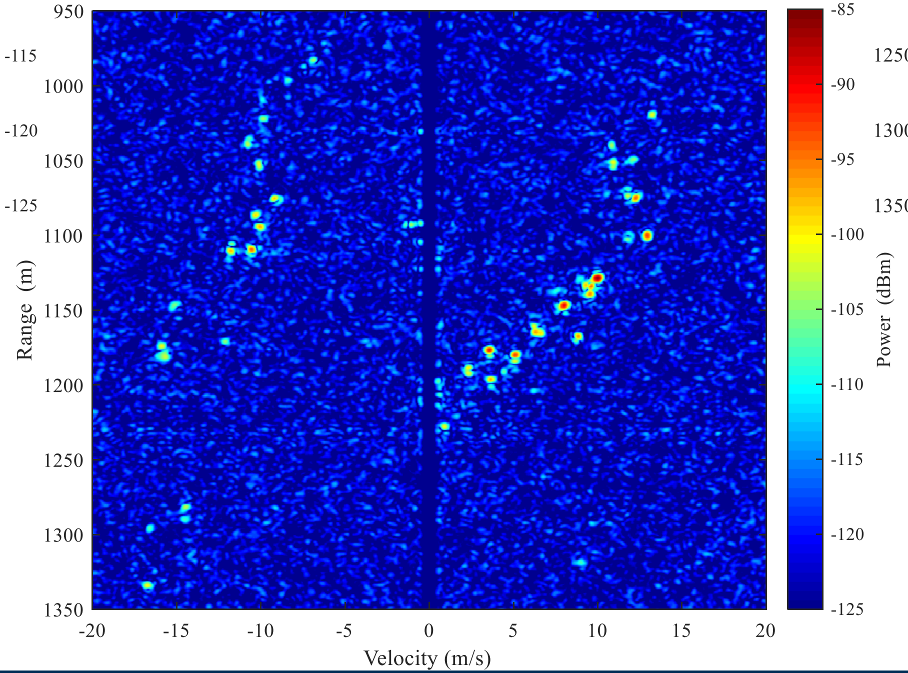

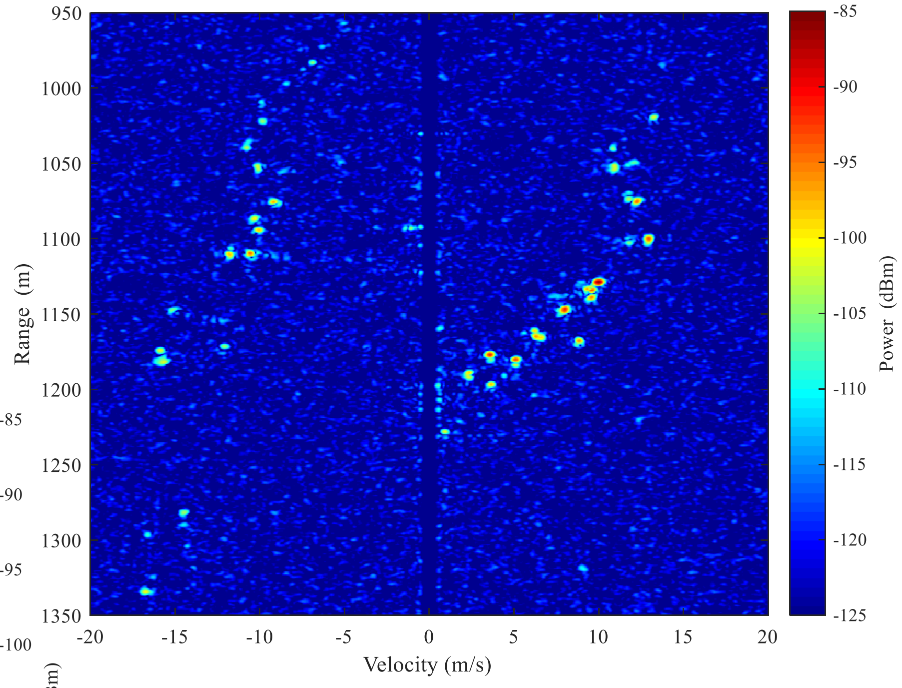

Fourier quasi-basis

Conclusions

- Due to the need for **oversampling**, parameterized FM waveforms possess **quasi-bases** (not full bases) having different attributes
  - Suggests different selections for different uses (e.g. required spectral containment)
  - Almost certain to be <u>other useful quasi-bases</u>

- Of the 3 examined here, **Fourier** tends toward **lower sidelobes** at the cost of spectral spreading, and **vice-versa** for **2nd order**, with 1st order in-between

- Other factors that can play a role for the particular waveforms generated are:
  - Nature of random initializations
  - Manner of imposing spectral containment
  - Alternative optimization methods/implementations

Questions?